DOI: 10.1002/ejoc.201000916

Guignardones A–C: Three Meroterpenes from *Guignardia mangiferae*

Wei Hua Yuan,[a] Min Liu,[a] Nan Jiang,[b] Zhi Kai Guo,[a] Jing Ma,[b] Jie Zhang,[a] Yong Chun Song,[a] and Ren Xiang Tan*[a]

Keywords: Circular dichroism / Configuration determination / Natural products / Structure elucidation / UV/Vis spectroscopy

Guignardones A (**1**), B (**2**), and C (**3**), which are three meroterpenes with frameworks most probably generated through a terpenoid shikimate pathway, were characterized by a combination of spectroscopic, X-ray crystallographic, and computational methods. The compounds were obtained from cultures of *Guignardia mangiferae* IFB-GLP-4 associated with normal *Ilex cornuta* leaves.

Introduction

Endophytes that inhabit normal plant tissues without affording any detectable symptoms are thought to be able to interact genetically with the host plants during long-term co-evolution. This differentiates them at least in part from microorganisms residing elsewhere in the biosynthesis and accumulation of the secondary metabolites with unknown structures, from which drug leads could be identified or optimized. As a follow-up to our previous investigation on the structure and function of symbiont-derived natural products,[1–4] we recognized that healthy *Ilex cornuta* leaves fostered a fungus that was subsequently identified as *Guignardia mangiferae* by analyzing its morphological character and its 18S rDNA sequence. Our preliminary investigation into the extract included ^{1}H NMR spectroscopic data acquisition and a bioassay, which suggested that the antibacterial extract derived from the fungal culture most likely contained terpene-like metabolite(s) with a molecular character similar to tricycloalternarenes (TCAs).[5,6] A detailed fractionation was therefore performed to isolate the three meroterpenes, named guignardones A (**1**), B (**2**), and C (**3**). We hereby wish to report the isolation, structure, and relevance of the three novel metabolites.

Results and Discussion

Guignardone A (**1**) was obtained as optically active colorless crystals. Its high-resolution ESI mass spectrum (HRESIMS) gave an $[M + Na]^+$ peak at m/z = 313.1407, which was indicative of a molecular formula of $C_{17}H_{22}O_4$ (calcd. for $C_{17}H_{22}O_4Na$ 313.1410) that retained seven degrees of unsaturation. DEPT and HMQC experiments revealed seventeen well-resolved resonance lines in the ^{13}C NMR spectrum of **1** that included two methyl, six methylene, three methine, and six quaternary carbon atoms. When correlated with the molecular formula, this observation implied that a hydrogen atom was also anchored on an oxygen atom. Furthermore, the tetracyclic nature of **1** could be determined from the two double bonds and one carbonyl group, which collectively accounted for only three degrees of unsaturation. This proposal was supported by analysis of the ^{1}H–^{1}H COSY, HMQC and HMBC spectra of **1** (Table 1). Briefly, the presence of substructure **1a** was demonstrated by the HMBC correlations observed for 11-H$_3$ (δ_H = 1.32 ppm) with C-9, C-10 and C-12, and of 17-H$_3$ (δ_H = 1.65 ppm) with C-14, C-15 and C-16 (Figure 1).

The partial structure **1b** was indicated by the HMBC correlations of 4-H (δ_H = 4.55 ppm) with C-2, C-3, C-5, C-6 and C-7, of 5-H (δ_H = 2.46 and 2.03 ppm) with C-1, C-3, C-5, C-6 and C-7, and of 7-H (δ_H = 3.81 and 3.49 ppm) with C-1, C-4, C-5 and C-6. The two substructures were combined in the formulated manner to generate the whole molecule of **1** on the basis of the HMBC correlation of 8-H (δ_H = 2.34 and 2.17 ppm) with C-1, C-2, C-3, C-9, C-10 and C-14. Finally, the structure of **1** (an analogue of TCAs) was confirmed by its X-ray diffraction analysis, which also established its relative configuration (Figure 2a).

The absolute stereochemical assignment of guignardone A (**1**) could not be readily accomplished from its CD spectrum (short of a comparable "model compound") and Mosher's method (lacking a secondary alcohol hydroxy group that could be acylated). However, guignardone A must be one of the two enantiomers (4*R*,6*S*,9*R*,10*S*,14*S*)-**1** or (4*S*,6*R*,9*S*,10*R*,14*R*)-**1** according to the relative configu-

[a] Institute of Functional Biomolecules, State Key Laboratory of Pharmaceutical Biotechnology, School of Life Sciences, Nanjing University,
Nanjing 210093, P. R. of China
Fax: +86-25-83302728
E-mail: rxtan@nju.edu.cn
[b] Institute of Theoretical and Computational Chemistry, Key Laboratory of Mesoscopic Chemistry of MOE, School of Chemistry and Chemical Engineering, Nanjing University,
Nanjing 210093, P. R. of China

Supporting information for this article is available on the WWW under http://dx.doi.org/10.1002/ejoc.201000916.

Table 1. ^{1}H (500 MHz) and ^{13}C (125 MHz) NMR spectroscopic data for **1**–**3** in $CDCl_3$.

	1				**2**		**3**	
	δ_H [ppm] (mult., *J* [Hz])	δ_C [ppm]	COSY	HMBC	δ_H [ppm] (mult., *J* [Hz])	δ_C [ppm]	δ_H [ppm] (mult., *J* [Hz])	δ_C [ppm]
1		198.8				198.7		195.1
2		102.9				102.7		104.3
3		172.8				174.0		169.6
4	4.55 (d, 5.4)	78.5	5-H	C-2,3,5,6,7	4.57 (d, 5.4)	78.4		77.6
5	2.46 (dd, 5.4, 10.8)	44.0	4-H	C-1,3,4,6,7	2.46 (dd, 5.4, 10.8)	44.0	2.47 (dd, 6.0, 10.9)	43.9
	2.03 (d, 10.8)				2.04 (d, 10.8)		1.98 (d, 10.9)	
6		81.7				81.7	4.46 (d, 6.0)	82.9
7	3.81 (d, 7.8)	70.6		C-1,4,5,6	3.81 (d, 7.8)	70.6	3.83 (d, 7.0)	73.5
	3.49 (d, 7.8)				3.52 (d, 7.8)		3.59 (d, 7.0)	
8	2.34 (dd, 17.1, 1.0)	15.5	9-H	C-1,2,3,9,10,14	2.64 (d, 17.0)	18.2	2.30 (d, 17.5)	15.9
	2.17 (overlap)				2.28 (dd, 17.0, 6.1)		2.15 (overlap)	
9	1.92 (m)	43.2	8,14-H	C-2,8,14,15	2.08 (m)	41.3	2.14 (m)	43.8
10		89.3				90.7		89.4
11	1.32 (s)	23.2		C-9,10,12	1.33 (s)	22.9	1.33 (s)	22.2
12	2.12 (m)	37.3	13-H	C-11,13	2.00 (m)	38.4	2.18 (m)	37.5
	1.80 (m)				1.64 (m)		1.88 (m)	
13	1.96 (m)	26.8	12,14-H	C-14	1.86 (m)	24.7	2.00 (m)	27.0
	1.55 (m)				1.55 (m)		1.60 (m)	
14	2.19 (m)	48.6	9,13-H	C-9,15	1.56 (m)	51.1	2.28 (m)	48.9
15		145.2				72.9		145.2
16	4.73 (m)	111.5		C-14,17	1.21 (s)	28.8	4.75 (s)	111.5
	4.61 (m)						4.65 (s)	
17	1.65 (s)	19.1		C-14,15,16	1.19 (s)	27.4	1.68 (s)	19.3

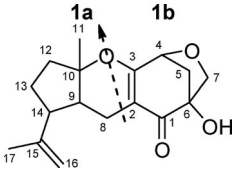

Figure 1. Structure and substructures (**a** and **b**) of **1**.

ration that was confirmed by the single-crystal X-ray diffraction analysis. Thus, a comparison was made between the experimental and calculated ECD spectra[7] after a UV correction of 16 nm (Figures 3 and S1) with the optimized structure by using the geometry determined from the X-ray analysis as the input for the structural optimization (Table S1). As illustrated in Figure 3, the calculated ECD curve for (4*S*,6*R*,9*S*,10*R*,14*R*)-**1** resembled the CD spectrum recorded for **1**, which is opposite to that calculated for (4*R*,6*S*,9*R*,10*S*,14*S*)-**1**. The first calculated positive Cotton effect at 216 nm can be assigned to the experimentally observed Cotton effect at 222 nm. The transitions from n-type (lone pair orbital of O) and σ-type (filled C–C orbital) to π*-type (antibonding C=O orbital in the carbonyl group) molecular orbitals (MOs), MO 73→79, contribute to this broad absorption band (Figure 4 and Table S2). The next

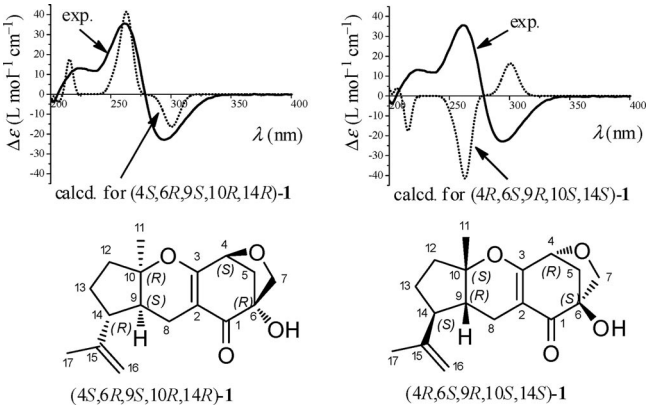

Figure 3. Comparison of the recorded ECD spectrum of **1** (solid line) with those calculated (dotted curve) for its enantiomers (4*S*,6*R*,9*S*,10*R*,14*R*)-**1** and (4*R*,6*S*,9*R*,10*S*,14*S*)-**1** after a UV correction of 16 nm.

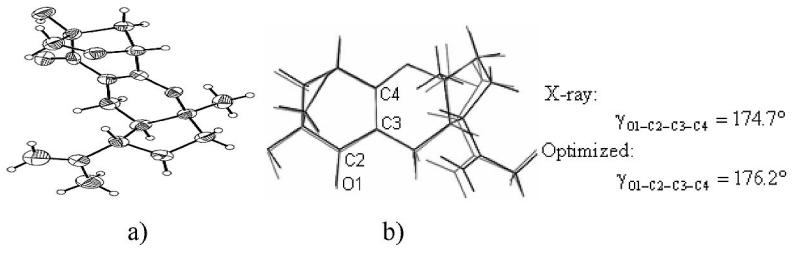

Figure 2. (a) X-ray crystal structure of **1**, and (b) superposition of the optimized geometry (gray) with the experimentally determined geometry (black).

positive Cotton effect was located at 263 nm, which could be assigned to the experimental absorption bands at 261 nm. The n→π* and π→π* excitations (MO 75→79 and MO 78→79), where n, π, and π* are the lone pair, bonding C=C, and antibonding C=O orbitals, respectively, play a dominant role. In the experimental CD spectrum, the negative band observed at 294 nm, which predominantly arises from π→π* and n→π* excitations (MO 78→79), is also well reproduced by the calculations (at 285 nm). Among these excitations, the electron-donating orbitals are the bonding C=C orbital of the ring framework and lone pair orbital of O, and the acceptor orbital is the antibonding C=O orbital of the carbonyl group. Thus, we concluded that the most likely absolute configuration of guignardone A is (4*S*,6*R*,9*S*,10*R*,14*R*).

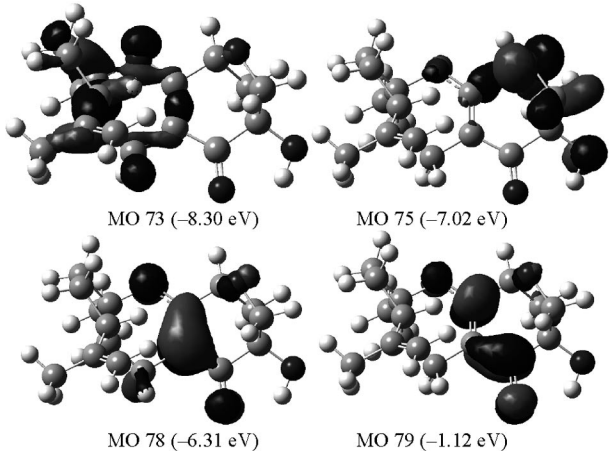

Figure 4. The most important orbitals of the optimized conformer of compound (4*S*,6*R*,9*S*,10*R*,14*R*)-**1**.

Guignardone B (**2**) was isolated as optically active colorless crystals. The HRESIMS of **2** exhibited a quasimolecular ion peak at *m*/*z* = 331.1513 $[M + Na]^+$, establishing a molecular formula of $C_{17}H_{24}O_5$ (calcd. $C_{17}H_{24}O_5Na$ 331.1516) with six degrees of unsaturation. The IR, ^1H and ^{13}C NMR spectroscopic data of **2** are quite close to those of **1**. However, metabolite **2** gave no IR absorption band around 1643 cm^{-1}. This observation, combined with the absence of carbon resonance lines at δ_C = 145.2 and 111.5 ppm, which are apparent in the ^{13}C NMR spectrum of **1** (see Table 1 in the Experimental Section), suggested that it was most likely a hydrate derivative of **1**. This proposal was reinforced by the upfield signals at δ = 72.9 (C-15) and 28.8 (C-16) ppm. The structure of **2** was further confirmed both by 2D NMR experiments (^1H–^1H COSY, NOESY, HMQC, and HMBC), and finally by single-crystal X-ray diffraction analysis (Figure 5a).

As in the case of **1**, the calculated ECD curve for (4*S*,6*R*,9*S*,10*R*,14*R*)-**2** was comparable with the experimentally acquired Cotton effect, highlighting their identity in stereochemistry (Figure 6).

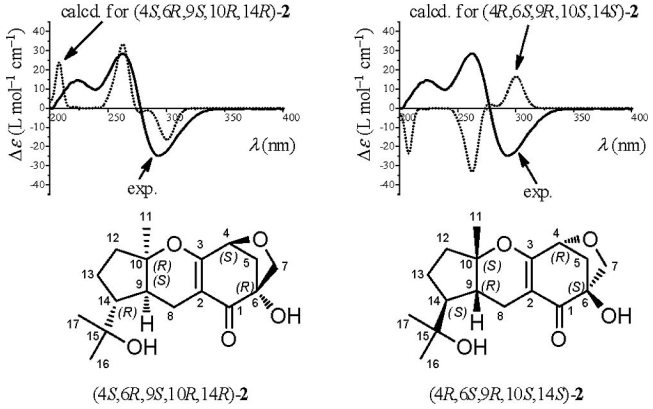

Figure 6. Comparison of the recorded ECD spectrum of **2** (solid line) with those calculated (dotted curve) for its enantiomers (4*S*,6*R*,9*S*,10*R*,14*R*)-**2** and (4*R*,6*S*,9*R*,10*S*,14*S*)-**2** after a UV correction of 16 nm.

Excitations from the lone pair orbitals of O and the σ-type molecular orbital to the π*-type MO of the carbonyl C=O and double C=C, play a dominant role in the absorbed bands. The electronic transitions of σ→π* (MO 76→84 and MO 77→84) contribute to the positive rotatory strengths at 208 nm. This is associated with the experimental Cotton effect at 223 nm (as shown in Table S4 and Figure 7). The next positive and negative Cotton effects at 262 and 300 nm can be assigned to the broad bands at about 262 and 294 nm in the acquired ECD spectrum, representing the excitations of n→π* and σ→π* (MO 81→84 and MO 82→84). Thus, we concluded that the absolute configuration of **2** was most likely (4*S*,6*R*,9*S*,10*R*,14*R*).

Guignardone C (**3**) was isolated as optically active colorless crystals. The HRESIMS of **3** exhibited a quasimolecular ion peak at *m*/*z* = 313.1408 $[M + Na]^+$, establishing a molecular formula of $C_{17}H_{22}O_4$ (calcd. $C_{17}H_{22}O_4Na$ 313.1410) with six degrees of unsaturation. The structure of **3** was elucidated by a set of 2D NMR spectra (^1H–^1H

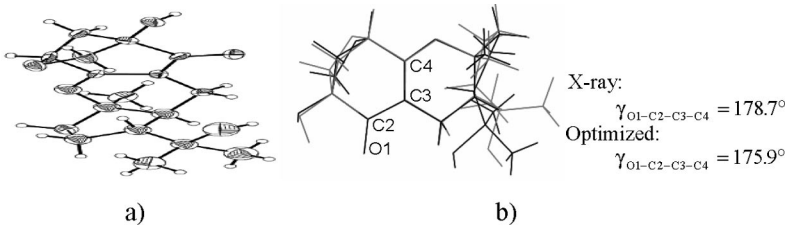

Figure 5. (a) X-ray crystal structure of **2**, and (b) superposition of the optimized geometry (gray) with the experimentally determined geometry (black).

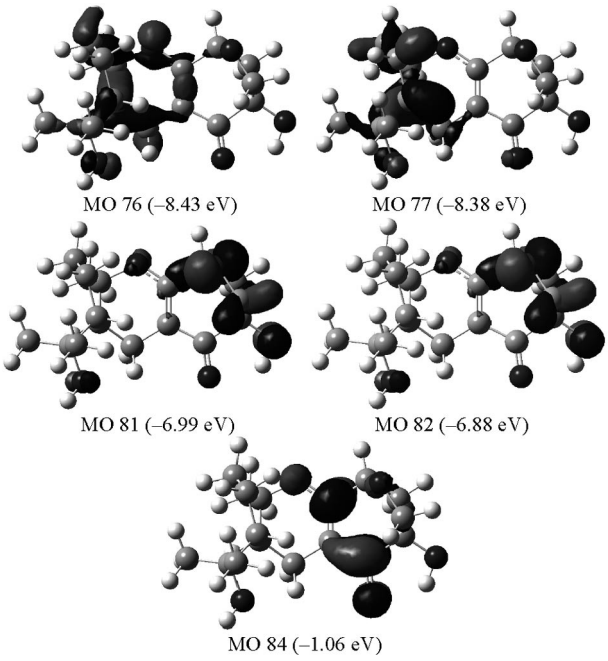

Figure 7. The most important orbitals of the optimized conformer of compound (4*S*,6*R*,9*S*,10*R*,14*R*)-**2**.

COSY, NOESY, HMQC, and HMBC), followed by single-crystal X-ray diffraction analysis (Figure 8a).

Concerning the absolute configuration, the calculated ECD curve for (4*R*,6*S*,9*S*,10*R*,14*R*)-**3** was comparable to the experimentally acquired Cotton effect (Figure 9).

The calculated positive Cotton effects at 258 and 319 nm could be assigned to the bands corresponding to those at 261 and 313 nm in the experimental ECD spectrum, respectively. The electronic excitations of the lone pair orbitals of O, the filled C–C and C=C molecular orbitals (designated as n_O, σ_{C-C} and $\pi_{C=C}$ MO, respectively) to π*-type C=O orbitals ($\pi^*_{C=O}$), MO 76→79, MO 78→79, and MO 77→79, contribute dominantly to these absorption bands, as shown in Table S6 and Figure 10. The electronic transitions of $n_O \rightarrow \pi^*$ and $\sigma_{C-H} \rightarrow \pi^*$ (MO 74→79) play an important role in the negative rotatory strengths at 228 nm. This is associated with the experimental Cotton effect at 224 nm. Thus, we concluded that the absolute configuration of **3** was most probably (4*R*,6*S*,9*S*,10*R*,14*R*).

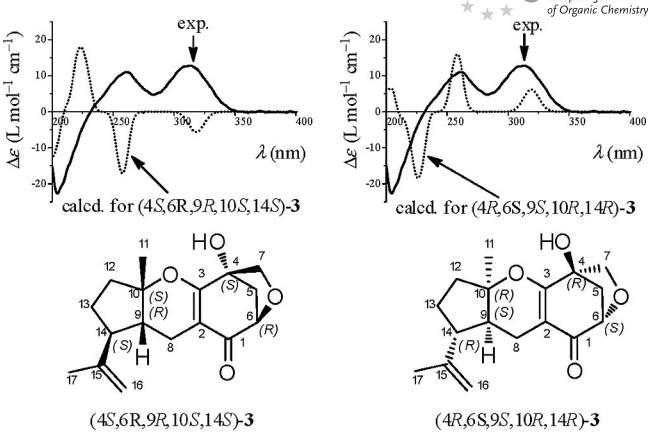

Figure 9. Attribution of the absolute configuration of guignardone C (**3**) enantiomers as (4*S*,6*R*,9*R*,10*S*,14*S*) and (4*R*,6*S*,9*S*,10*R*,14*R*) by comparing the experimental (solid line) and calculated (dotted line) ECD spectra after a UV correction of 16 nm.

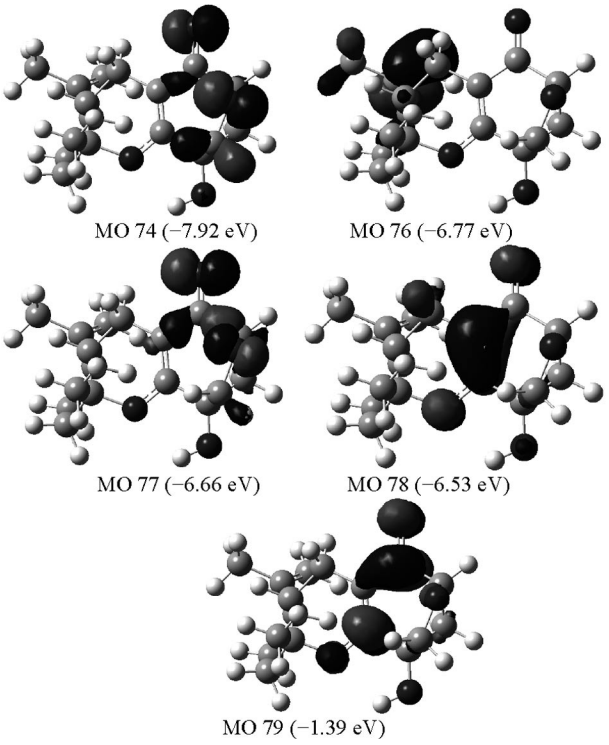

Figure 10. The most important orbitals of the optimized conformer of (4*R*,6*S*,9*S*,10*R*,14*R*)-**3**.

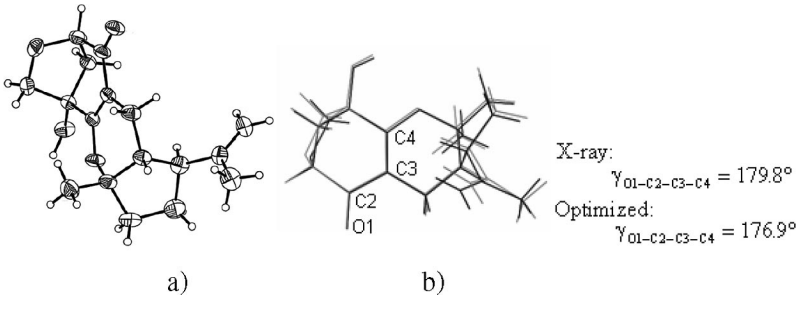

Figure 8. (a) X-ray crystal structure of **3**, and (b) superposition of the optimized geometry (gray) with the experimentally determined geometry (black).

The good agreement between the calculated and experimental ECD spectra in solution indicated that the DFT-optimized conformer was dominant in solution, presumably due to the conformational rigidity of the tetracyclic nucleus. As illustrated in Figures 2b, 5b, and 8b, the DFT-optimized geometries for **1**–**3** are close to the corresponding X-ray structures. In addition, the dihedral angles of O1–C1–C2–C3 (designated as $\gamma_{O1–C2–C3–C4}$) in **1**–**3** are very close to 180.0°, indicating that the α,β-unsaturated ketone moiety can be an inherently chiral chromophore.

As suggested in Scheme 1, we hypothesized that a precursor **X** would be a potential intermediate that, through alternative cyclization patterns of the substructures **a** and **b**, would lead to the generation of guignardones A–C (**1**–**3**). Although the 10-hydroxy group has similar access to both the 1- and 3-ketone groups, the content of guignardone A (**1**) in the culture broth was demonstrated to be much higher than that of guignardone C (**3**), in spite of the transformation of guignardone A into metabolite **2**. This could be due to the fact that C-4 and C-6 exert differing degrees of steric hindrance on the neighboring carbonyl groups.

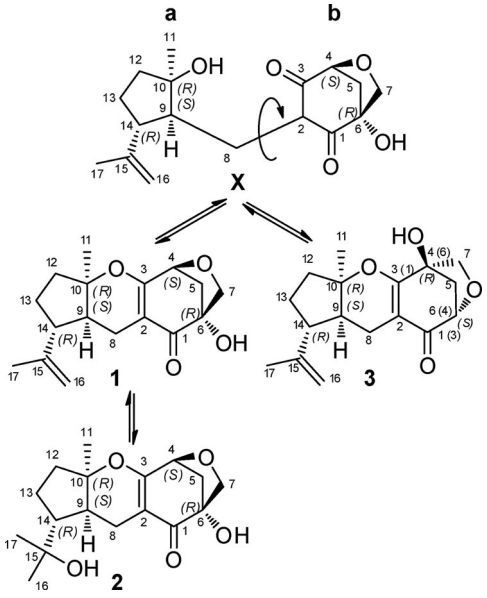

Scheme 1. The relevance of guignardones A–C (**1**–**3**).

Conclusions

The title fungus *Guignardia mangiferae*, which resides inside *Ilex cornuta* leaves, has been demonstrated to be a reliable producer of three antibacterial metabolites designated as guignardones A–C (**1**–**3**). These metabolites have similar molecular architectures to TCAs, and are most probably generated through a terpenoid-shikimate pathway.

Experimental Section

General Instrumentation and Reagents: As detailed in our previous communications.[1–4]

Strain and Cultivation: The strain IFB-glp-4 was isolated from the leaf of *Ilex cornuta* collected in December 2007 from the back hill of Nanjing Forestry University, China. The strain was identified as *Guignardia mangiferae* by comparing the morphological character and 18S rDNA sequence with that of a standard record. A voucher specimen is deposited in our laboratory. The fresh mycelium of IFB-glp-4 was inoculated in a 1 L flask containing 400 mL of modified Czapek's medium (consisting of 3 g of $NaNO_3$, 1 g of K_2HPO_4, 0.5 g of KCl, 0.5 g of $MgSO_4·7H_2O$, 0.01 g of $FeSO_4·7H_2O$, 30 g of sucrose, and 1 g of yeast in 1 L of distilled water). Cultivation was carried out at 28 °C with an agitation of 150 rpm for 11 d. The procedure was repeated until sufficient biomass was accumulated.

Isolation and Characterization Data of Metabolites 1–3: A filtrate of the culture broth (40 L) was extracted exhaustively with EtOAc. The EtOAc extract was concentrated under reduced pressure to give a brown oily residue (7.0 g), which gave seven fractions upon silica gel column chromatography (petroleum ether/acetone, gradient 100:1→1:1). The third fraction (diluted with petroleum ether/acetone, 10:1) was subjected to ODS CC (CC: column chromatography) (MeOH/H_2O, 80:20) to give of **1** (65 mg, 98%) as a colorless crystalline solid. The fourth fraction (diluted with petroleum ether/acetone, 5:1) was subjected to ODS CC (MeOH/H_2O, 60:40) to give **2** (16 mg, 98%) and **3** (12 mg, 98%) as colorless crystalline solids. The ^1H (500 MHz) and ^{13}C (125 MHz) and 2D NMR spectra of **1**–**3** in $CDCl_3$ are listed in Table 1.

Guignardone A (1): Colorless crystals; m.p. 94–96 °C. UV (MeOH): λ_{max} = 263 nm. $[\alpha]_D^{20}$ = 42 (*c* = 0.30, acetone). IR (KBr): $\tilde{\nu}_{max}$ = 3397.8, 3071.3, 2950.9, 2905.0, 1654.7, 1618.9, 1461.9, 1382.1, 1303.5, 1242.3, 1171.7, 1121.3, 1027.5, 978.1, 891.8 cm^{-1}. MS (ESI): *m*/*z* = 313 $[M + Na]^+$, 289 $[M – H]^-$. HRESIMS: calcd. for $C_{17}H_{22}O_4Na$ $[M + Na]^+$ 313.1410; found 313.1407. For ^1H and ^{13}C NMR spectroscopic data, see Table 1.

Guignardone B (2): Colorless crystals; m.p. 160–162 °C. UV (MeOH): λ_{max} = 264 nm. $[\alpha]_D^{20}$ = 67 (*c* = 0.76, acetone). IR (KBr): $\tilde{\nu}_{max}$ = 3419.8, 2968.8, 2941.2, 2891.3, 1655.0, 1616.2, 1469.8, 1447.1, 1405.7, 1377.0, 1362.7, 1302.0, 1253.5, 1175.1, 1118.1, 1024.7, 976.6, 899.4 cm^{-1}. MS (ESI): *m*/*z* = 331 $[M + Na]^+$, 307 $[M – H]^-$. HRMSESI: calcd. for $C_{17}H_{24}O_5Na$ $[M + Na]^+$ 331.1516; found 331.1513. For ^1H and ^{13}C NMR spectroscopic data, see Table 1.

Guignardone C (3): Colorless crystals; m.p. 99–101 °C. UV (MeOH): λ_{max} = 266 nm. $[\alpha]_D^{20}$ = 489 (*c* = 0.07, acetone). IR (KBr): $\tilde{\nu}_{max}$ = 3376.4, 3075.3, 2968.8, 2876.0, 1648.5, 1606.4, 1442.6, 1397.1, 1334.3, 1258.6, 1173.9, 1157.7, 1099.4, 1045.6, 918.0 cm^{-1}. MS (ESI): *m*/*z* = 313 $[M + Na]^+$, 289 $[M – H]^-$. HRMSESI: calcd. for $C_{17}H_{22}O_4Na$ $[M + Na]^+$ 313.1410; found 313.1408. For ^1H and ^{13}C NMR spectroscopic data, see Table 1.

Computational Details: Density functional theory (DFT) at the B3LYP/6-31G(d) level was employed to optimize the geometries of the guignardones A–C (**1**–**3**) in CH_3OH solvent. To evaluate the solvent effects on the electronic structures of the studied systems, the solute was treated with a quantum chemistry method through the PCM model (dielectric constant ε = 32.63). Then, the corresponding excited-state calculations were performed on the ground-state optimized geometries. Time-dependent DFT calculations in combination with PCM model (TD-DFT/PCM) with the same basis set were carried out to calculate the spin-allowed excitation energy and rotatory strength of the lowest 120 excited states. The final ECD spectra were obtained according to Equations (1) and (2):[8]

$$\Delta\varepsilon(\lambda) = \sum_n \Delta\varepsilon_n \exp\left[-\left(\frac{\lambda-\lambda_n}{\Delta\lambda_n}\right)^2\right] \quad (1)$$

$$\Delta\varepsilon_n = \frac{\lambda_n R_n}{22.94\sqrt{\pi}\Delta\lambda_n} \times 10^{40} \quad (2)$$

where $\Delta\varepsilon_n$ is the peak intensity ($L\,mol^{-1}\,cm^{-1}$), R_n is the rotatory strength (10^{-40} cgs), λ_n is the wavelength (nm) of the nth transition, and $\Delta\lambda_n$ is the half-width at $1/e$ of peak maximum (cm^{-1}). Here we used a half-width $\Delta\lambda_n = \lambda_n^2\Delta\tilde{\nu}$ with $\Delta\tilde{\nu} = 1200\ cm^{-1}$ for guignardones A–C (**1**–**3**). The systematic errors in the prediction of the wavelength and excited-state energies are compensated for by employing UV correction.[9,10] All calculations were performed with the Gaussian 03 program.[11]

X-ray Structure Determination: CCDC-713773 (**1**), -747079 (**2**), and -752598(**3**) contains the supplementary crystallographic data for this paper. These data can be obtained free of charge from The Cambridge Crystallographic Data Centre via www.ccdc.cam.ac.uk/data_request/cif.

Supporting Information (see footnote on the first page of this article): For optimized structural information on (4*S*,6*R*,9*S*,10*R*,14*R*)-**1**, (4*S*,6*R*,9*S*,10*R*,14*R*)-**2**, and (4*R*,6*S*,9*S*,10*R*,14*R*)-**3**, see Tables S1, S3, and S5, respectively; for the TD-DFT results (200 nm $< \lambda <$ 400 nm) for the optimized conformers, see Tables S2, S4, and S6, respectively; for the calculated UV spectra, see Figures S1, S2, and S3, respectively.

Acknowledgments

The work was co-financed by grants for R. X. T. from the Ministry of Science and Technology (MOST) (2009ZX09501-013) and the National Natural Science Foundation of China (NSFC) (30821006), and for W. H. Y. from the China Postdoctoral Science Foundation Funded Project (200904501078) and the Jiangsu Planned Projects for Postdoctoral Research Funds (0901021C).

[1] Y. L. Zhang, H. M. Ge, H. Dong, Q. Xu, S. H. Li, J. Li, J. Zhang, Y. C. Song, R. X. Tan, *Angew. Chem. Int. Ed.* **2008**, *47*, 5823–5826.
[2] L. Shen, R. H. Jiao, Y. H. Ye, X. T. Wang, C. Xu, Y. C. Song, H. L. Zhu, R. X. Tan, *Chem. Eur. J.* **2006**, *12*, 5596–5602.
[3] L. Shen, Y. H. Ye, X. T. Wang, H. L. Zhu, C. Xu, Y. C. Song, H. Li, R. X. Tan, *Chem. Eur. J.* **2006**, *12*, 4393–4396.
[4] R. H. Jiao, S. Xu, J. Y. Liu, H. M. Ge, H. Ding, C. Xu, H. L. Zhu, R. X. Tan, *Org. Lett.* **2006**, *8*, 5709–5712.
[5] Y. Kono, J. M. Gardner, Y. Suzuki, H. Kondo, S. Takeuchi, *J. Pestic. Sci.* **1989**, *14*, 223–228.
[6] a) B. Liebermann, R. Ellinger, W. Güther, W. Ihn, H. Gallander, *Phytochemistry* **1997**, *46*, 297–303; b) R.-P. Nussbaum, W. Güther, S. Heinze, B. Liebermann, *Phytochemistry* **1999**, *52*, 593–599; c) B. Liebermann, R.-P. Nussbaum, W. Güther, *Phytochemistry* **2000**, *55*, 987–992; d) B. Liebermann, R.-P. Nussbaum, W. Güther, J.-M. Teuscher, *Phytochemistry* **2001**, *56*, 551–557.
[7] a) P. J. Stephens, D. M. McCann, E. Butkus, S. Stončius, J. R. Cheeseman, M. J. Frisch, *J. Org. Chem.* **2004**, *69*, 1948–1958; b) P. J. Stephens, D. M. McCann, F. J. Devlin, J. R. Cheeseman, M. J. Frisch, *J. Am. Chem. Soc.* **2004**, *126*, 7514–7521; c) D. M. McCann, P. J. Stephens, *J. Org. Chem.* **2006**, *71*, 6074–6098; d) P. J. Stephens, D. M. McCann, F. J. Devlin, A. B. Smith III, *J. Nat. Prod.* **2006**, *69*, 1055–1064; e) P. J. Stephens, J. J. Pan, F. J. Devlin, *J. Org. Chem.* **2007**, *72*, 3521–3536; f) P. J. Stephens, F. J. Devlin, *J. Org. Chem.* **2007**, *72*, 4707–4715.
[8] A. Jiemchooroj, P. Norman, *J. Chem. Phys.* **2007**, *126*, 134102.
[9] G. Bringmann, S. Busemann, in *Natural Product Analysis: Chromatography, Spectroscopy, Biological Testing* (Eds.: P. Schreier, M. Herderich, H.-U. Humpf, W. Schwab), Vieweg, Wiesbaden, **1998**, pp. 195–211.
[10] G. Bringmann, T. Bruhn, K. Maksimenka, Y. Hemberger, *Eur. J. Org. Chem.* **2009**, 2717–2727.
[11] M. J. Frisch, G. W. Trucks, H. B. Schlegel, G. E. Scuseria, M. A. Robb, J. R. Cheeseman, J. A. Montgomery Jr., T. Vreven, K. N. Kudin, J. C. Burant, J. M. Millam, S. S. Iyengar, J. Tomasi, V. Barone, B. Mennucci, M. Cossi, G. Scalmani, N. Rega, G. A. Petersson, H. Nakatsuji, M. Hada, M. Ehara, K. Toyota, R. Fukuda, J. Hasegawa, M. Ishida, T. Nakajima, Y. Honda, O. Kitao, H. Nakai, M. Klene, X. Li, J. E. Knox, H. P. Hratchian, J. B. Cross, V. Bakken, C. Adamo, J. Jaramillo, R. Gomperts, R. E. Stratmann, O. Yazyev, A. J. Austin, R. Cammi, C. Pomelli, J. W. Ochterski, P. Y. Ayala, K. Morokuma, G. A. Voth, P. Salvador, J. J. Dannenberg, V. G. Zakrzewski, S. Dapprich, A. D. Daniels, M. C. Strain, O. Farkas, D. K. Malick, A. D. Rabuck, K. Raghavachari, J. B. Foresman, J. V. Ortiz, Q. Cui, A. G. Baboul, S. Clifford, J. Cioslowski, B. B. Stefanov, G. Liu, A. Liashenko, P. Piskorz, I. Komaromi, R. L. Martin, D. J. Fox, T. Keith, M. A. Al-Laham, C. Y. Peng, A. Nanayakkara, M. Challacombe, P. M. W. Gill, B. Johnson, W. Chen, M. W. Wong, C. Gonzalez, J. A. Pople, *Gaussian 03*, Revision D.01, Gaussian, Inc., Wallingford, CT, **2004**.

Received: June 27, 2010
Published Online: October 5, 2010

